Electrochemical evidence of the reorientation of alkynes on trimetallic clusters during a two-electron reduction

Domenico Osella, Lubomir Pospisil, and Jan Fiedler

Organometallics, **1993**, 12 (8), 3140-3144• DOI: 10.1021/om00032a042 • Publication Date (Web): 01 May 2002

Electrochemical Evidence of the Reorientation of Alkynes on Trimetallic Clusters during a Two-Electron Reduction

Domenico Osella*

Dipartimento di Chimica Inorganica, Chimica Fisica e Chimica dei Materiali, Università di Torino, Via P. Giuria 7, 10125 Torino, Italy

Lubomir Pospisil and Jan Fiedler

J. Heyrovsky Institute of Physical Chemistry and Electrochemistry, Dolejskova 3, 18223 Prague, Czech Republic

Received July 20, 1992

The electrochemical two-electron reduction of isoelectronic and isostructural alkyne clusters of iron and osmium has been investigated by fast-scan cyclic voltammetry. Both $Fe_3(CO)_9$-(EtC≡CEt) and $Os_3(CO)_7(Ph_2PCH_2PPh_2)$(PhC≡CPh) undergo a two-electron reduction. While $Fe_3(CO)_9$(EtC≡CEt) is reduced in two separate one-electron waves, $Os_3(CO)_7(Ph_2PCH_2PPh_2)$-(PhC≡CPh) displays a single two-electron wave. Fast-scan voltammetry detects one additional adsorption post-peak for the iron cluster which, under certain experimental conditions, gives rise to apparent anomalous shapes of voltammograms. Differences in electrochemical pattern of iron and osmium title compounds are interpreted on the basis of follow-up and concomitant isomerization reactions with respect to the first electron transfer, respectively.

Introduction

Redox processes involving the simultaneous transfer of two (or more) electrons can occur when the second electron transfer is thermodynamically easier then the first electron uptake. This class of redox processes, besides its practical importance in reductions of O_2, CO_2, N_2, etc., has been actively investigated with the aim of identifying the factors which contribute to overcoming the electrostatic hindrance of the second charge-transfer step.[1] Geometrical rearrangements are considered as one of the possible mechanisms which could lead to generation of an intermediate that is reduced at potentials more positive than for the parent compound.[2]

The $Fe_3(CO)_9$(alkyne) derivatives are formally electronically unsaturated (46e). Shilling and Hoffmann[3] predicted that the alkyne orientation over the Fe_3 triangle in the model compound $Fe_3(CO)_9$(HC≡CH) is a consequence of the different energies of the frontier MO's. Thus, the perpendicular (⊥) orientation is preferred for the neutral 46e species, but a parallel (∥) orientation is forecast for the corresponding 48e species, namely the $[Fe_3(CO)_9(HC{\equiv}CH)]^{2-}$ dianion. A similar behavior can also be predicted using the polyhedral skeletal electron pair (PSEP) approach.[4] Indeed, $Fe_3(CO)_9$(EtC≡CEt) (1) (Figure 1) exhibits two fully reversible one-electron-reduction processes.[5] Upon reduction 1 produces a stable diamagnetic dianion, so that the parallel coordination of the alkyne in 1^{2-} has been unambiguously proved by NMR spectroscopy.[5] The back-donation from the two equivalent metal atoms to the alkyne plays an important role in the preference for the perpendicular coordination of the organic chain over the metallic triangle.[6] Indeed, the analogous $M_3(CO)_9$(⊥-PhC≡CPh) (M = Ru, Os) derivatives turn out to be highly unstable or elusive, due to the higher electronegativities of such metals.[7] It is, however, possible to obtain the stable $Os_3(CO)_7(Ph_2PCH_2PPh_2)$(⊥-$PhC_2Ph$) derivative (2) (Figure 1), where the presence of a good σ-donor, poor π-acceptor diphosphine provides the two equivalent osmium atoms with sufficient electron density for efficient back-donation.[8] A homologous compound, namely $Ru_3(CO)_7(Ph_2PCH_2PPh_2)$(⊥-$PhC_2Ph$), has been recently characterized by Lavigne and co-workers.[9]

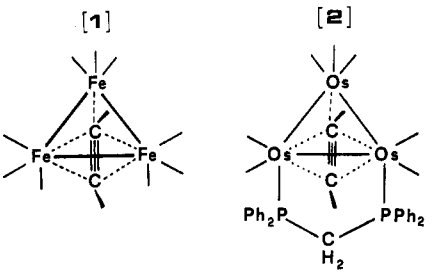

Figure 1. Sketch of the structures of $Fe_3(CO)_9$(EtC≡CEt) (1) and $Os_3(CO)_7(Ph_2PCH_2PPh_2)$(PhC≡CPh) (2). The CO ligands and the alkyne substituents are omitted for clarity.

The electrochemical scenario of 2 is similar to that of 1, but a single-step two-electron reduction is observed instead of two subsequent, one-electron reductions. Chemical and spectroscopic evidence indicates a parallel geometry in $(2)^{2-}$.[10]

(1) Kalyanasundaram, K.; Gratzel, M.; Pelizzetti, E. *Coord. Chem. Rev.* **1986**, *69*, 67.
(2) Geiger, W. E. *Prog. Inorg. Chem.* **1985**, *33*, 275.
(3) (a) Shilling, B. E. R.; Hoffmann, R. *J. Am. Chem. Soc.* **1979**, *101*, 3456. (b) Shilling, B. E. R.; Hoffmann, R. *Acta Chem. Scand., Ser. B* **1979**, *150*, 123.
(4) Wade, K. *Adv. Inorg. Chem. Radiochem.* **1976**, *18*, 1.
(5) Osella, D.; Gobetto, R.; Montangero, P.; Zanello, P.; Cinquantini, A. *Organometallics* **1986**, *5*, 1247.
(6) (a) Busetti, V.; Granozzi, G.; Aime, S.; Gobetto, R.; Osella, D. *Organometallics* **1984**, *3*, 1510. (b) Aime, S.; Bertoncello, R.; Busetti, V.; Gobetto, R.; Granozzi, G.; Osella, D. *Inorg. Chem.* **1986**, *25*, 4004.
(7) (a) Tachikawa, M.; Shapley, J. R.; Pierpont, C. G. *J. Am. Chem. Soc.* **1975**, *97*, 7172. (b) Clauss, A. D.; Shapley, J. R.; Wilson, S. R. *J. Am. Chem. Soc.* **1981**, *103*, 7387.
(8) Clucas, J. A.; Dolby, P. A.; Harding, M. M., Smith, A. K. *J. Chem. Soc., Chem. Commun.* **1987**, 1829.
(9) Rivomanana, S.; Lavigne, G.; Lugan, N.; Bonnet, J. J. *Inorg. Chem.* **1991**, *30*, 4112.

0276-7333/93/2312-3140$04.00/0

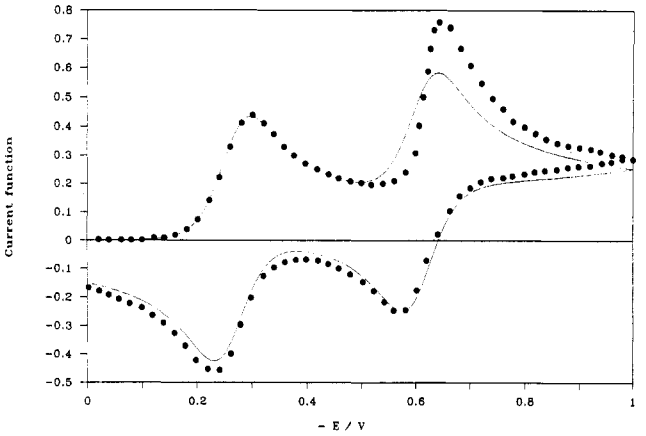

Figure 2. Cyclic voltammetric response (●) of an acetone solution of 1 (6×10^{-4} M) containing tetrabutylammonium hexafluorophosphate (0.1 M) as supporting electrolyte at scan rate 1 V s^{-1} and the simulated curve (—) for a simple EE mechanism, assuming $E°_1 = -0.260$ V and $E°_2 = -0.620$ V.

An attempt to detect this rearrangement upon reduction in 1 and 2 by electrochemical techniques is the subject of the present paper.

Results and Discussion

Mechanism of Reduction of 1. The two redox steps observed in acetone solution of $Fe_3(CO)_9(EtC{\equiv}CEt)$ at a Hg electrode have formal potentials $E°_1 = -0.260$ and $E°_2 = -0.585$ V vs SCE. Coulometry indicates a chemically reversible one-electron transfer in each step.[5] The shape of the cyclic voltammogram recorded at 1 V s^{-1} in an ordinary manner (without special attention to timing described below) is shown in Figure 2, together with a theoretical curve for an uncomplicated two-step reduction (EE mechanism). Obviously the experimental wave form differs from the simulated one mainly because the second peak is to some extent higher than the first one and the wave shape is much steeper. The difference in the wave shape is qualitatively analyzed after the transformation of the cyclic voltammogram to a semiintegrated voltammogram (sometimes called "neo-polarogram")[11-13] which permits the application of diagnostic criteria usual for the polarographic technique (Figure 3). From several algorithms able to perform the semiintegration, we have used the Riemann–Liouville[12] transform of the order $-1/2$. The "log plot" analysis[14] of the first wave in the forward scan bears the features of an uncomplicated charge-transfer process with reversible character. The slope of the cathodic log plot, 60.8 mV/decade, is in good agreement with the value predicted for a Nernstian redox reaction. The more negative part of the log-plot curve merges with an asymptote corresponding to the charge-transfer coefficient $\alpha = 0.57$. The log-plot analysis of the second reduction wave (the *apparent* half-wave potential is –0.625 V) leads to a conclusion that it has a "super-Nernstian" slope (steeper than 59 mV) which may originate from kinetic or adsorption effects. The reoxidation waves obtained upon the reversal of the voltage sweep show no significant sign

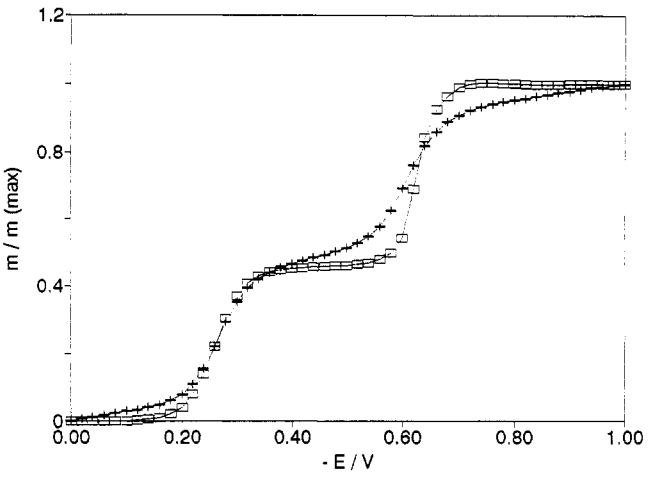

Figure 3. Semiintegrated experimental voltammogram of data given in Figure 2 for the forward scan (□) and for the reverse scan (+).

Scheme I

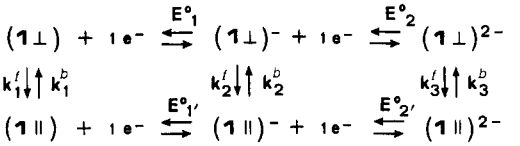

of mechanistic complications. The attempt goal of the analysis of electrochemical data is the allocation of the perpendicular to parallel geometrical rearrangement, *i.e.* whether the isomerization occurs after the first electron transfer (ECE mechanism), or after the reduction to the dianion (EEC mechanism), or possibly in a way concomitant with the electrode reaction E_CE or EE_C mechanism).[15]

The existence of two isomers requires consideration of Scheme I, first proposed by Jacq.[18] For the present system six redox states, $1\perp$, $1\perp^-$, $1\perp^{2-}$, $1\parallel$, $1\parallel^-$, and $1\parallel^{2-}$, are to be considered, where the symbols $\perp$ and $\parallel$ indicate isomers with perpendicular and parallel configurations of alkyne, respectively. The horizontal arrows indicate the redox reactions, whereas the vertical ones indicate the chemical isomerization between various redox forms (Scheme I).

The heterogeneous kinetic parameters of the first row will be denoted as $k°_1$, α_1, $E°_1$ and $k°_2$, α_2, $E°_2$ for $1\perp/1\perp^-$ and $1\perp^-/1\perp^{2-}$ redox couples, respectively. The second-row parameters we will distinguish by primes, *e.g.* $k°_1'$, α_1', $E°_1'$ and $k°_2'$, α_2', $E°_2'$ for $1\parallel/1\parallel^-$ and $1\parallel^-/1\parallel^{2-}$ redox couples, respectively. Our task is to find the most probable pathway through which the form $1\parallel^{2-}$ can be generated by reduction of $1\perp$, and then transformed back upon oxidation. On a priori chemical knowledge of the system we can disregard several rate constants from Scheme I. Only the $1\parallel^{2-}$ form was characterized, whereas $1\parallel$ was not detected at all, even as a transient in a previous VT-NMR study;[19] therefore, $k^f_1 = 0$. The stability of a parallel

(10) Brown, P. M.; Dolby, P. A.; Harding, M.; Mathews, A. J.; Smith, A. K.; Osella, D.; Arbrun, M.; Gobetto, R.; Raithby, P. R.; Zanello, P. *J. Chem. Soc., Dalton Trans.* **1993**, 827.
(11) Oldham, K. B. *Anal. Chem.* **1972**, *44*, 196.
(12) Oldham, K. B.; Zoski, G. D. *Anal. Chem.* **1980**, *52*, 2116.
(13) Soong, F. C.; Maloy, J. T. *J. Electroanal. Chem. Interfacial Electrochem.* **1983**, *153*, 29.
(14) Ruzic, I. *J. Electroanal. Chem. Interfacial Electrochem.* **1974**, *52*, 331.
(15) We employ the nomenclature that E represents a heterogeneous electron transfer and C a homogeneous chemical reaction (actually an isomerization reaction). Therefore, the symbol ECE represents a stepwise process in which a redox system undergoes a two-electron-transfer process with the interposition of the geometrical rearrangement.[16] In contrast, the notation E_CE indicates the geometrical rearrangement occurs concomitant with the first charge transfer.[17]
(16) Tulyathan, B.; Geiger, W. E. *J. Am. Chem. Soc.* **1985**, *107*, 5960.
(17) Finke, R. G.; Voegell, R. H.; Laganis, E. D.; Boekelheide, V. *Organometallics* **1983**, *2*, 347.
(18) Jacq, J. *J. Electroanal. Chem. Interfacial Electrochem.* **1971**, *29*, 149.
(19) Granozzi, G.; Tondello, E.; Casarin, M.; Aime, S.; Osella, D. *Organometallics* **1983**, *2*, 439.

Scheme II

$$(1\perp) + 1e^- \overset{E^\circ_1}{\rightleftharpoons} (1\perp)^- + 1e^- \overset{E^\circ_2}{\rightleftharpoons} (1\perp)^{2-}$$
$$\uparrow k_2^b \qquad\qquad k_3^f \downarrow$$
$$(1\parallel)^- + 1e^- \overset{E^\circ_{2'}}{\rightleftharpoons} (1\parallel)^{2-}$$

Scheme III

$$(1\perp) + 1e^- \overset{E^\circ_1}{\rightleftharpoons} (1\perp)^- + 1e^- \overset{E^\circ_2}{\rightleftharpoons} (1\perp)^{2-}$$
$$k_2^f \downarrow \uparrow k_2^b$$
$$(1\parallel)^- + 1e^- \overset{E^\circ_{2'}}{\rightleftharpoons} (1\parallel)^{2-}$$

Scheme IV

$$(1\perp) + 1e^- \overset{E^\circ_1}{\rightleftharpoons} (1\perp)^- + 1e^- \overset{E^\circ_2}{\rightleftharpoons} (1\perp)^{2-}$$
$$\uparrow k_1^b \qquad\qquad k_3^f \downarrow$$
$$(1\parallel) + 1e^- \overset{E^\circ_{1'}}{\rightleftharpoons} (1\parallel)^- + 1e^- \overset{E^\circ_{2'}}{\rightleftharpoons} (1\parallel)^{2-}$$

dianion allows us to consider that the equilibrium $1\perp^{2-} \rightleftarrows 1\parallel^{2-}$ is strongly shifted to the right and hence $k^f_3 \gg k^b_3$. It remains to to be seen which of the remaining four rate constants are high enough to determine the reaction path.

Three reaction schemes listed below have to be considered.

Mechanism I. The isomerization from the perpendicular to the parallel configuration takes place after the transfer of two electrons as an EEC mechanism, whereas the regeneration of the perpendicular form occurs after the loss of the first electron from the dianion (Scheme II).

Mechanism II. The isomerization from the perpendicular to the parallel configuration takes place after the transfer of the first electron as an ECE mechanism, and the regeneration of the perpendicular form follows the same path after the loss of one electron from the dianion (Scheme III).

Mechanism III. The isomerization from the perpendicular to the parallel configuration takes place after the transfer of the second electron as an EEC mechanism, and the regeneration of the perpendicular form occurs after removal of two electrons during reoxidation (Scheme IV).

The analysis of Scheme I thus simplifies to the determination of just two rates of chemical isomerization between parallel and perpendicular isomers. In this way the number of adjustable parameters is substantially reduced, giving a better chance of finding the actual mechanism. The three mechanisms given above were simulated numerically using the finite difference method of Feldberg.[20] The requirement for an acceptable fit of simulated and experimental data in the range of scan rates 0.05–1 V s^{-1} was the reproduction of the following experimental features: (a) an increase of the second cathodic wave, (b) a higher "steepness" of the second reduction wave, and (c) an overall chemical reversibility of the reduction–oxidation cycle.

Mechanism II was rejected because it generates wave forms without increased steepness of the second wave as well as with overly large shifts of maxima with scan rate variation. Between the remaining schemes, mechanism I better approaches the steep shape of the second wave; however, a complete fit was never achieved due to the instability of calculations at higher rates. Further experimental evidence described below disclosed adsorption effects detectable at very short measurement time which proved to be a more important phenomenon.

(20) Feldberg, S. W. *J. Phys. Chem.* **1971**, *75*, 2377.

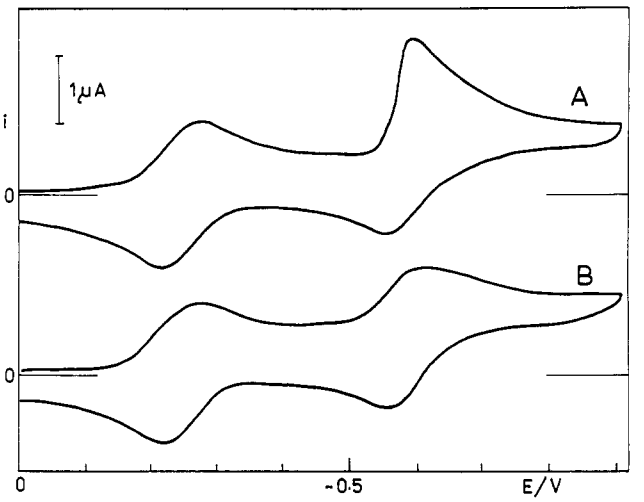

Figure 4. Cyclic voltammetry of 5.2×10^{-4} M 1 in 0.1 M tetrabutylammonium hexafluorophosphate in acetone at the scan rate 1 V s^{-1}: (A) scan after a 30-s wait at the initial potential; (B) scan starting immediately after the formation of the mercury electrode.

A super-Nernstian slope of the second wave can indeed be caused by adsorption effects. The following experiments have confirmed that adsorption of 1 on the mercury electrode in acetone solvent plays an important role. In a routinely performed voltammetric experiment there is a certain short delay between the formation of the stationary mercury drop electrode and the start of the potential scan. Such a delay is present not only in manual operations but even in computer-controlled experiments. We have modified the software in such a way that the delay could be precisely varied. The cyclic voltammogram recorded with a zero delay and a relatively slow scan rate (from 0.1 to 1.0 V s^{-1}) exhibits all features of an uncomplicated EE process with Nernstian shape of both reduction peaks (Figure 4, curve B). Thus, the anomalous "steepness" of the second reduction wave (Figure 4, curve A) has disappeared, indicating the participation of a time-dependent adsorptive accumulation of the reactant $1\perp$. These striking features require a detailed study, because the isomerization can modify not only the electron-transfer properties but also the geometrical orientation of the electroactive molecule at the electrode.

By the recording of cyclic voltammograms at high scan rates, the existence of adsorbed species at the electrode surface has been confirmed. At scan rate of 10 V s^{-1} a sharp adsorption post-peak is observed at the peak potential of about –0.7 V (Figure 5). The height of the maximum strongly depends on the accumulation time at the initial potential and on the scan rate. The higher the scan rate and the longer accumulation time, the higher the maximum. At the scan rate 100 V s^{-1} the post-peak (labeled in Figure 6 as P_1) is clearly discernible even with no accumulation time (curve 1 in Figure 6). The assignment of P_1 as an adsorption post-peak is suggested also by its symmetrical shape. The adsorption at the starting potential was verified by the phase-sensitive admittance measurements in ac polarography checking the change of the double-layer capacitance with respect to that of the blank solution.

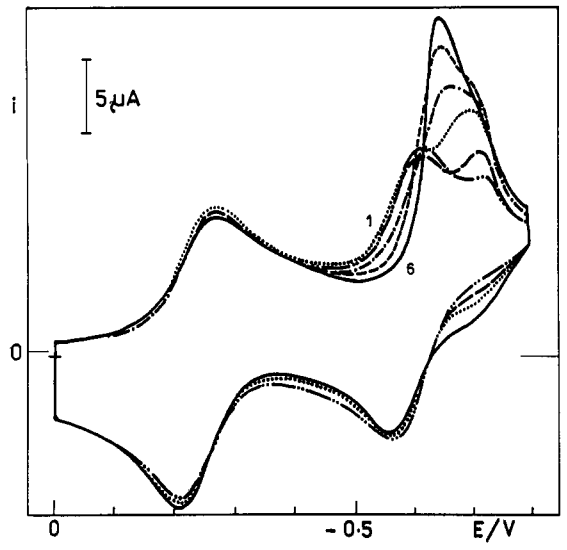

Figure 5. Cyclic voltammetry of an acetone solution of 1 (5.2×10^{-4}) containing tetrabutylammonium hexafluorophosphate (0.1 M) at the scan rate 10 V s^{-1} with different accumulation times at the initial potential (0.0 V *vs* SCE): (1) 0 s; (2) 5 s; (3) 15 s; (4) 20 s; (5) 25 s; (6) 30 s. Only curves 1 and 6 are labeled.

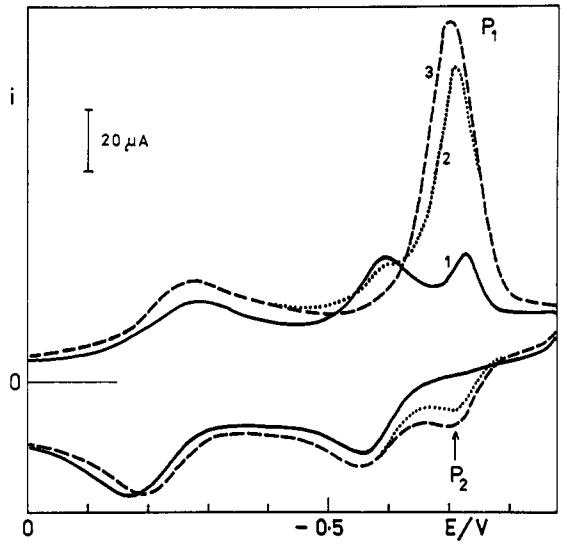

Figure 6. Cyclic voltammetry of an acetone solution of 1 (5.2×10^{-4} M) containing tetrabutylammonium hexafluorophosphate (0.1 M) at the scan rate 100 V s^{-1} with different accumulation times at the initial potential (0.0 V *vs* SCE): (1) 0 s; (2) 3 s; (3) 5 s. Note the appearance of the peak P_2 at the same potential of that of the post-peak P_1.

The existence of a post-peak in cyclic voltammetry is a firm indication of adsorption of the oxidized form.[21] However, the picture described above is anomalous in several aspects. The peak P_1 appears as a post-peak of the second reduction step, though the accumulation occurs at potentials prior to the first reduction process and the first reduction wave itself is unaffected. If the adsorption post-peak P_1 were due to the adsorption of the partially reduced form $1\perp^-$, the dependence on the scan rate should be reversed: high potential scan rates should lower the post-peak P_1 due to insufficient time for the adsorption process of any intermediate. We then suppose that the parent cluster $1\perp$ is adsorbed from the solution onto the electrode surface to an extent depending on the waiting time prior to the start of the potential scan. Both redox forms involved in the first electron-transfer step, $1\perp$ and $1\perp^-$, must have almost identical adsorption properties; this fact leaves the first redox wave practically unchanged.[22] Provided that the change sought in alkyne coordination (from perpendicular to parallel) takes place after the first electron uptake, it is very probable that the unadsorbed fraction of $1\perp^-$ changes its geometry faster than the surface-bound one. This could explain the two regular EE waves observed at slow scan rate (under conditions of negligible accumulation times), because the potential change is slow enough that even the adsorbed fraction of $1\perp^-$ changes to a parallel configuration. At high scan rate the post-peak P_1 increases since the adsorbed intermediate $1\perp^-$ can no longer change its geometry due to a finite rate of the isomerization step. The interpretation of P_1 in terms of a surface-bound redox change is supported by the appearance of an anodic peak P_2 visible at 100 V s^{-1} (Figure 6) located at the same potential as P_1 (*i.e.* –0.72 V) having specular symmetry, both features typical of adsorbed redox pairs.[22]

We further confirmed this interpretation by performing similar series of experiments in different solvents. Experiments in acetonitrile still indicate moderate adsorption; the effects are smaller, and the P_1 maximum appears at potentials 0.2 V more negative than the second reduction wave. In contrast, the cyclic voltammogram of 1 in dichlormethane yields two uncomplicated one-electron waves even at the scan rate 100 V s^{-1} without any influence of the initial accumulation time. Indeed, in previous work on the electrochemical behavior of the $Fe_3(CO)_9$(alkyne) series in CH_2Cl_2 at both Pt and Hg electrodes (employing moderate scan rates) no adsorption was found.[5] In agreement with voltammetric data, the admittance measurements in ac polarography confirm adsorption at the initial potentials in the case of acetone and acetonitrile; in contrast dichloromethane efficiently eliminates such an adsorption.

Interestingly enough, adsorption is usually considered as an obstacle in the electrochemical measurements. In the actual case, the surface activity of the adsorbed redox pairs could be used for the detection of the isomerization step otherwise too difficult to observe.

Mechanism of Reduction of 2. In contrast to the case of iron cluster 1, the reduction of $Os_3(CO)_7(Ph_2PCH_2PPh_2)(PhC{\equiv}CPh)$ (**2**) proceeds as a single two-electron process (Figure 7). The process is chemically reversible, but the cathodic–anodic wave separation with scan rate corresponds to an electrochemically *quasi*-reversible process. At a Hg electrode and in acetone, the peak current ratio is still 1.0 but the peak separation is as high as 155 mV at a scan rate of 0.2 V s^{-1}. The formal electrode potential $E^{\circ\prime}$, estimated as the average of peak potentials (E_p), is –0.805 V, and the *apparent* transfer coefficient, α, is 0.33 (estimated from the half-width of the cathodic peak for $n_{app} = 2$). The semiintegrated voltammogram (Figure 8) shows a single two-electron cathodic and anodic wave system. The numerical simulations of cyclic voltammograms in the range of scan rates from 0.05 to 1.0 V s^{-1} were performed for several mechanisms. Once again, one can obtain several good fits with experiments. One such possibility is to employ mechanism III with $E^\circ_1 > E^\circ_2$ and $E^\circ_1{}' < E^\circ_2{}'$ and select kinetic parameters for the best fit. Alternatively, one can obtain an equally good fit for a simpler E_CE scheme in which the isomerization

(21) Wopschall, R. H.; Shain, I. *Anal. Chem.* **1967**, *39*, 1514.

(22) Marcus, R. A. *Annu. Rev. Phys. Chem.* **1964**, *15*, 155.

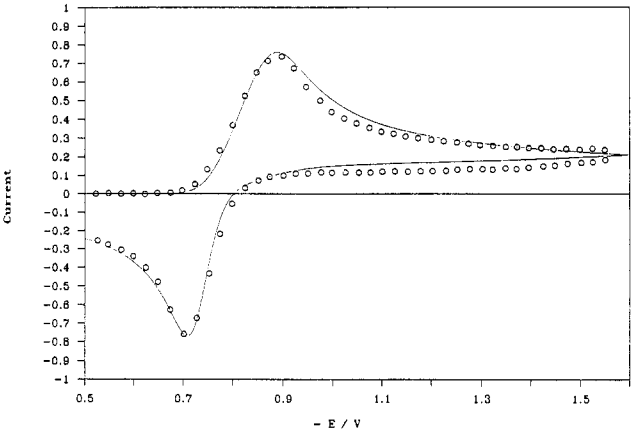

Figure 7. Cyclic voltammetric response (O) of an acetone solution of **2** (6×10^{-4} M) containing tetrabutylammonium hexafluorophosphate (0.1 M) at the scan rate 0.2 V s^{-1} and a simulated curve (—) for an E_CE mechanism, assuming the following parameters: $E^\circ_1 = -0.855$ V, $k^\circ_1 = 0.10$ cm s^{-1}, $\alpha = 0.55$ (for the first electron transfer); $E^\circ_2 = -0.690$ V, $k^\circ_2 = 0.50$ cm s^{-1}, $\alpha = 0.50$ (for the second electron transfer).

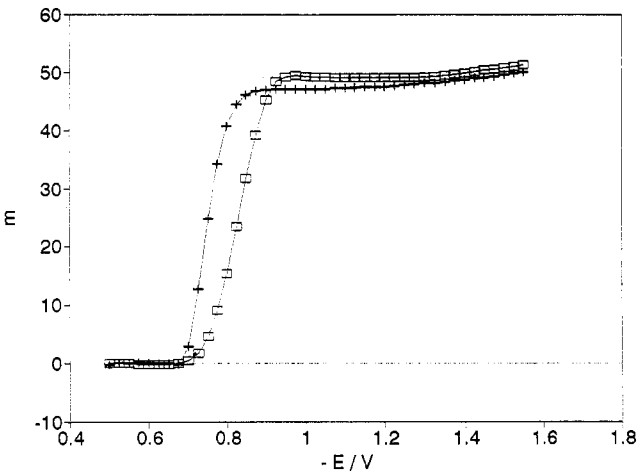

Figure 8. Semiintegrated experimental voltammogram of data given in Figure 7 for the forward (□) and for the reverse scan (+).

change takes place concomitantly with the first electron transfer (Scheme V).

An energetic barrier due to the internal bond change should accompany the electron transfer.[22,23] In such a case, the second electron transfer is characterized by a more positive redox potential with a higher heterogeneous rate constant. Reaction mechanisms based on the structural change concomitant with the first electron transfer were observed in several homogeneous[24] and heterogeneous[25] charge-transfer reactions. Concomitant isomerizations were proven in carbonyl and π-arene complexes of group 8 metals.[2] In analogy with these studies, we favor the interpretation of the observed behavior in terms of a concomitant structural change against more complex schemes, which include a larger number of adjustable kinetic parameters. The comparison of the experimental curve with the simulation obtained within the E_CE model is shown in Figure 7, and the agreement is quite satisfactory, assuming the following parameters: $E^\circ_1 = -0.855$ V, $k^\circ_1 = 0.10$ cm s^{-1}, $\alpha = 0.55$ (for the first electron transfer); $E^\circ_2 = -0.690$ V, $k^\circ_2 = 0.50$ cm s^{-1}, $\alpha = 0.50$ (for the second electron transfer).

Scheme V

$$(\mathbf{2}\perp) + 1e^- \underset{}{\overset{E^\circ_1}{\rightleftharpoons}} (\mathbf{2}\parallel)^- + 1e^- \overset{E^\circ_2}{\rightleftharpoons} (\mathbf{2}\parallel)^{2-}$$

The fit of these parameters was checked with experimental data in the range of scan rates from 0.05 to 1.0 V s^{-1}.

Experimental Section

Clusters **1** and **2** were synthesized according to previously published procedures.[5,8] Their purity was checked by IR and ^{1}H NMR spectroscopy. Acetone was Burdick and Jackson "distilled in glass" purity grade. Tetrabutylammonium hexafluorophosphate was used as supporting electrolyte. The electrochemical measurements were made using a laboratory-built electrochemical system consisting of a fast-rise-time potentiostat and a triangular voltage generator. An EG&G lock-in amplifier, Model 5350, used for admittance measurements was interfaced to a personal computer via the IEEE-interface card PcLab, Model 748. Fast cyclic voltammograms were recorded by means of a Tektronix Waveform Digitizer 5D10 oscilloscope plug-in unit and transferred to the computer memory. Experiments were performed at 20 °C in a thermostated electrochemical three-electrode cell with the SCE reference electrode separated from the test solution by a salt bridge. The potentials were checked with respect to $FeCp_2$, added as internal standard. Under the actual experimental conditions the $FeCp_2^{0/+}$ couple is located at +0.48 V vs SCE in acetone.[26] The working electrode was a valve-operated static mercury dropping electrode (SMDE, Laboratorní Přístroje, Prague, Czech Republic). The voltage scan rate was synchronized with the formation of a fresh electrode surface. The auxiliary electrode was a mercury pool or a cylindrical platinum net. Oxygen was removed from the solution by passing a stream of argon or nitrogen.

Appendix

The algorithm used here is based on the Riemann–Liouville[12] transform of the order $-1/2$, which yields the desired transformation. The calculation of the semiintegral $m(t)$ from experimentally recorded currents $i(t)$ during the potential scan is based on the property

$$\mathcal{L}\{m(t)\} = s^q \mathcal{L}\{i(t)\}$$

relating the Laplace ($\mathcal{L}$) transform of $i(t)$ to its semiintegral via multiplication by a power $q = -1/2$ of frequency s. On this principle one can design a recursive digital filter which handles an array of digital cyclic voltammograms as if it were multipled by $q - 1/2$ in the frequency domain. This approach speeds up the calculation to a fraction of a second.[27]

Acknowledgment. We thank the Consiglio Nazionale delle Richerche (CNR, Rome) for a visiting grant (to L.P.), Johnson Matthey Ltd. for a generous loan of OsO_4, and P. A. Loveday (University Chemical Laboratory, Cambridge, U.K.) for high-pressure synthesis of $Os_3(CO)_{12}$. We wish to thank Professors W. E. Geiger (University of Vermont) and C. Amatore (Ecole Normale Supérieure, Paris) for their interest.

OM920436Q

(23) Marcus, R. A. *J. Chem. Phys.* **1965**, *43*, 679.
(24) Endicott, J. F.; Kumar, K.; Ramasami, T.; Rotzinger, F. P. In *Progress in Inorganic Chemistry*; Lippard, S. J., Ed.; Wiley: New York, 1983; Vol. 30.
(25) Bowyer, W. J.; Geiger, W. E. *J. Electroanal. Chem. Interfacial Electrochem.* **1988**, *239*, 253.
(26) Geiger, W. E. In *Organometallic Radical Processes*; Trogler, W. C., Ed.; Elsevier: Amsterdam, 1990.
(27) Pajkossy, T.; Nyikos, L., private communication.